May 17th, 9:00 AM

Effects of Weir with an Opening on Bed Morphology and Flow Patterns

T. Ohmoto
ohmoto@kumamoto-u.ac.jp

Hirotaka UNE
167d8807@st.kumamoto-u.ac.jp

Recommended Citation

Ohmoto, T. (2018). Effects of Weir with an Opening on Bed Morphology and Flow Patterns. Daniel Bung, Blake Tullis, 7th IAHR International Symposium on Hydraulic Structures, Aachen, Germany, 15-18 May. doi: 10.15142/T3ND24 (978-0-692-13277-7).

7th International Symposium on Hydraulic Structures Aachen, Germany, 15-18 May 2018
ISBN: 978-0-692-13277-7 DOI: 10.15142/T3ND24

Effects of Weir with an Opening on Bed Morphology and Flow Patterns

T. Ohmoto[1] & H. Une[1]
[1]*Department of Civil and Environmental Engineering, Kumamoto University,*
Kurokami, Chuo-ku, Kumamoto, JAPAN
E-mail: ohmoto@kumamoto-u.ac.jp

Abstract: *The scouring or depositing downstream of submerged weirs with an opening is a sediment phenomena resulting from the interaction of the three-dimensional turbulent flow field around the structure and the moveable sand bed. This paper presents the experimental study on the downstream channel bed due to a weir with an opening, paying attention to the effects of relative overflow depth on local scouring around the structure, sand bars, and three-dimensional flow patterns. The experiments were conducted under the clear-water scour condition for an equilibrium scour hole. The experimental results show that local scouring and sand bar development downstream of the submerged weirs decrease with relative overflow depth and turn out strongly paired cellular secondary currents.*

Keywords: *Weir with an opening, local scouring, sand bar, three-dimensional turbulent flow, cellular secondary currents*

1. Introduction

It has been pointed out that stream-crossing structures such as dams and weirs tend to interrupt the continuity of natural streams, destroy the diversity of the physical and biological environments, and reduce natural disturbances. In the United States, more than 500 weirs and dams have already been removed in order to remove deteriorated dams including weirs and improve river environments (Graf, 2002). In 2011, the dam on the Elwha River in the state of Washington in the western United States was removed. It has been reported that the ecosystem of the river has been recovering to a sound state as can be seen, for example, from the native species recovery (East et al., 2015). In a gravel-bed river, sediment, if supplied in an appropriate manner, penetrates the spaces between gravel particles so as to stabilize the river bed. Sediment flowing into pools in a river section where bed slope is steep and water flows through a series of riffles and pools transforms the pool bed surface and, thereby, facilitates the establishment of new epiphytic algae. (Doyle et al., 2005; Kibler et al., 2011).

The Arase Dam is a hydroelectric power generation dam located in the town of Sakamoto, Yatsushiro City, about 20 km upstream from the estuary of the Kuma River flowing through the southern part of Kumamoto Prefecture in Japan. The dam was removed by the phased removal method starting in fiscal year 2012. The Enterprise Bureau of the Kumamoto Prefectural Government, therefore, has been conducting a study on the effect of dam removal on river bed processes and the river environment. On March 31, 2010, the gates of the Arase Dam were opened. Since the height of the dam to its crest is 11.3 m, it is essentially categorized as weir removal. (Task Committee for the Arase Dam Removal, 2017).

Guan et al. (2013) discussed scour patterns of a river bed immediately downstream of a weir and flow patterns and turbulence characteristics of such a river channel, and pointed out that secondary currents occur immediately downstream of the weir, showing clearly discernible three-mensional flow structures, even if the weir is uniform in shape in the cross-stream direction.

Melville (1997) reviewed past studies on bridge piers and abutments, and presented an empirical formula for calculating the maximum scour depth.

Ohmoto and Hirakawa (1999) elucidated the effect of groin direction on secondary currents, main stream velocity, and river bed processes. Ishigaki and Baba (1999) investigated the relationship between flow around a plate with footing and local scouring, and showed that local scouring around a plate with footing is governed by spiral flow (strong secondary flow occurring from the end of the footing) instead of horseshoe-shaped vortices occurring in front of the footing.

Only a few studies looked at the effect of partial removal of a weir on river bed processes.

In the experiments they conducted, Zhang et al. (2012) placed various weirs with an opening in a flume bedded with various materials with different grain sizes and specific gravities, and investigated scour characteristics of the bed immediately upstream of the weir in an overflow condition and local flows near the weir. Sumida et al. (2015) used a flume with a relatively large aspect ratio and examined the effects of the shape and size of weir opening on river bed processes immediately upstream of the weir and the formation of flow channels due to scouring. Not many studies, however, have looked at the influence of a weir with an opening on river bed processes in the channel downstream of the weir, and few studies have dealt with scour and deposition characteristics of and flow structure over a river bed immediately downstream of a partially removed weir.

Before looking at a dynamic river bed, this study focuses on a static equilibrium bed. In this study, the effect of relative overflow depth on river bed processes, basic characteristics of sandbars downstream of a weir, and the three-dimensional structure of flow over the river bed are examined.

2. Experimental Apparatus and Method

A series of experiments was conducted by using a 10-meter-long, 40-centimeter-wide, 20-centimeter-high recirculating variable-slope acrylic flume.

As shown in Figure 1, a weir with a 10-centimeter-wide central opening was placed at a distance of 5 m from the upstream end of the flume. A movable bed of uniform thickness (within the range from 3 cm to 10.5 cm), which was determined according to relative overflow depth, composed of silicate sand having an average grain size of 1.7 mm and a coefficient of uniformity of 1.50, was laid in the 4.5-meter-long section upstream of the weir and the 4.5-meter-long section downstream. The bottom of the opening zone was composed of silicate sand, and scouring was allowed to occur. The bed upstream of the weir was made 1 cm higher than the bed downstream of the weir.

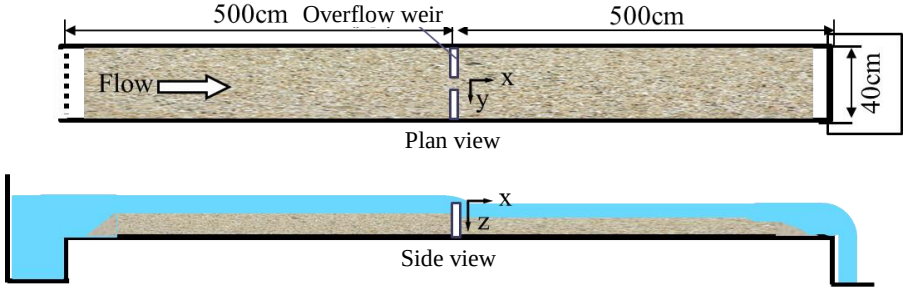

Figure 1. Experimental channel

Table 1 shows the conditions for the movable bed experiments. Since this study focuses on a static equilibrium bed, flow rates were set so that the tractive force remains below the critical level in the upstream and downstream sections outside the zone of influence of the weir. Relative overflow depth is a value obtained by dividing overflow depth by weir height.

In the experiments, silica sand was laid on the flume bed up to a bed height determined according to relative overflow depth, and the weir at the downstream end was operated for a predetermined water depth under the conditions of a constant flow rate (Q = 4.3 l/s) and a constant channel slope (I = 1/500). In all cases, bed height was measured after the bed reached a state of equilibrium following 24 hours or more. Relative overflow height was systematically varied at cross-sectional average flow velocities of about 10 cm/s and 20 cm/s at points outside the zone of local scour due to the weir. In the table, U is the cross-sectional average flow velocity at a point 3 m upstream of the weir, overflow depth H, weir height Dw, and the critical flow velocity U_{cr} for bed material. K_I corresponds to the flow intensity K factor proposed by Melville (1997).

The origin of the coordinate system is located at the center of the initial sand bed in the flume where the opening is located. The right-hand coordinate system has an x-axis in the flow direction, a y-axis in the spanwise direction, and a z-axis in the vertical downward direction. Their flow velocity components are represented by u, v, and w; their time average components by U, V, and W; and their variable components by u', v', and w'. Water level and river bed height were measured with a point gauge and an ultrasonic water level sensor, respectively.

Table 1. Experimental conditions for the movable bed

Case	U(cm/s)	Fr	K_I	H(cm)	D_w(cm)	H/D_W
1-1	10	0.1	0.23	0	11	0
1-2				2	9	0.22
1-3				3	8	0.38
1-4				4	7	0.57
1-5				5	6	0.83
1-6				5.5	5.5	1.0
2-1	20	0.27	0.47	1	4.5	0.22
2-2				1.5	4	0.38
2-3				2	3.5	0.57
2-4				2.5	3	0.83
2-5				2.7	2.8	0.97
2-6				3	2.5	1.2

For the investigation of flow mechanisms, point measurement and multi-point simultaneous measurements of water surface profile and flow velocity were made in Case 2-4 shown in Table 1. Surface flow measurement was made by the Particle Image Velocimetry (PIV) method using a video camera system capable of multi-point simultaneous measurements of flow velocity, and the point measurement of flow velocity was made with one-component and two-component electromagnetic current meters. In the flow velocity measurement by the PIV method, water surface profile was video-recorded from directly above the flume for a period of 20 seconds, and nylon particles having a particle size of 100 μm and a specific gravity of 1.02 were used as a tracer. Visualization image data were recorded on a computer's hard disk in the form of 59.94 fp (frames per second) 1920×1080-pixel black-and-white image data and were processed by the PIV method. The 100Hz output signals from the electromagnetic current meters were processed with an analog-to-digital converter, and data for a total of 4,096 data sets were statistically processed for each measuring point.

3. Experimental Results

3.1. Riverbed Variation in an Equilibrium State Under Clear-Water Scour Condition

Figures 2 and 3 show scour and sedimentation contours at cross-sectional average flow velocities of 10 cm/s and 20 cm/s, respectively. The contour figures show the amounts of changes (in millimeters) from the initial flat bed figures. At the cross-sectional average flow velocity of 10 cm/s, significant scouring can be seen in the regions immediately upstream and downstream of the weir opening when relative overflow depth is zero (non-overflow condition). Scour width is ±10 cm in the cross-stream direction and −8 cm to +13 cm in the flow direction, indicating spatial scales roughly two times as large as the initial water depth of 11 cm. As shown, when viewed two-dimensionally, scour width depth tends to be greater on the upstream side than in the downstream side. The maximum scour depth, which occurs at the end of the weir, is about 60 mm.

In the section downstream of the weir, sandbars which are conspicuously oblong in plan view emerge near the right and left banks. The maximum sediment thickness is about 40 mm, which is about two-thirds of the maximum scour depth, and the centers of the sandbars are located at around x = 20 cm downstream of 3.2the weir and y = ±15 cm in the cross-stream direction. In the mid-channel zone, scouring tends to occur at x = 0 to 15 cm and sedimentation tends to occur at x = 15 to 30 cm.

At the cross-sectional average flow velocity of 10 cm/s and the relative overflow depths of 0.22 and 0.38, scouring is reduced considerably and occurs only in the region near the end of the weir, and sedimentation zones shaped like the Japanese katakana character "ha" (ハ) can be seen on the downstream side of the weir. Significant scouring does not occur in the mid-channel zone near the weir opening, and the channel bed immediately downstream shows a gradual rise.

At the cross-sectional average flow velocity of 20 cm/s, scouring occurs near the weir opening in a concentrated manner, and it can be seen that the two-dimensional spread and depth of scour decrease as relative overflow depth increases. It can also be seen that scour depth is greater on the upstream side of the weir than on the downstream

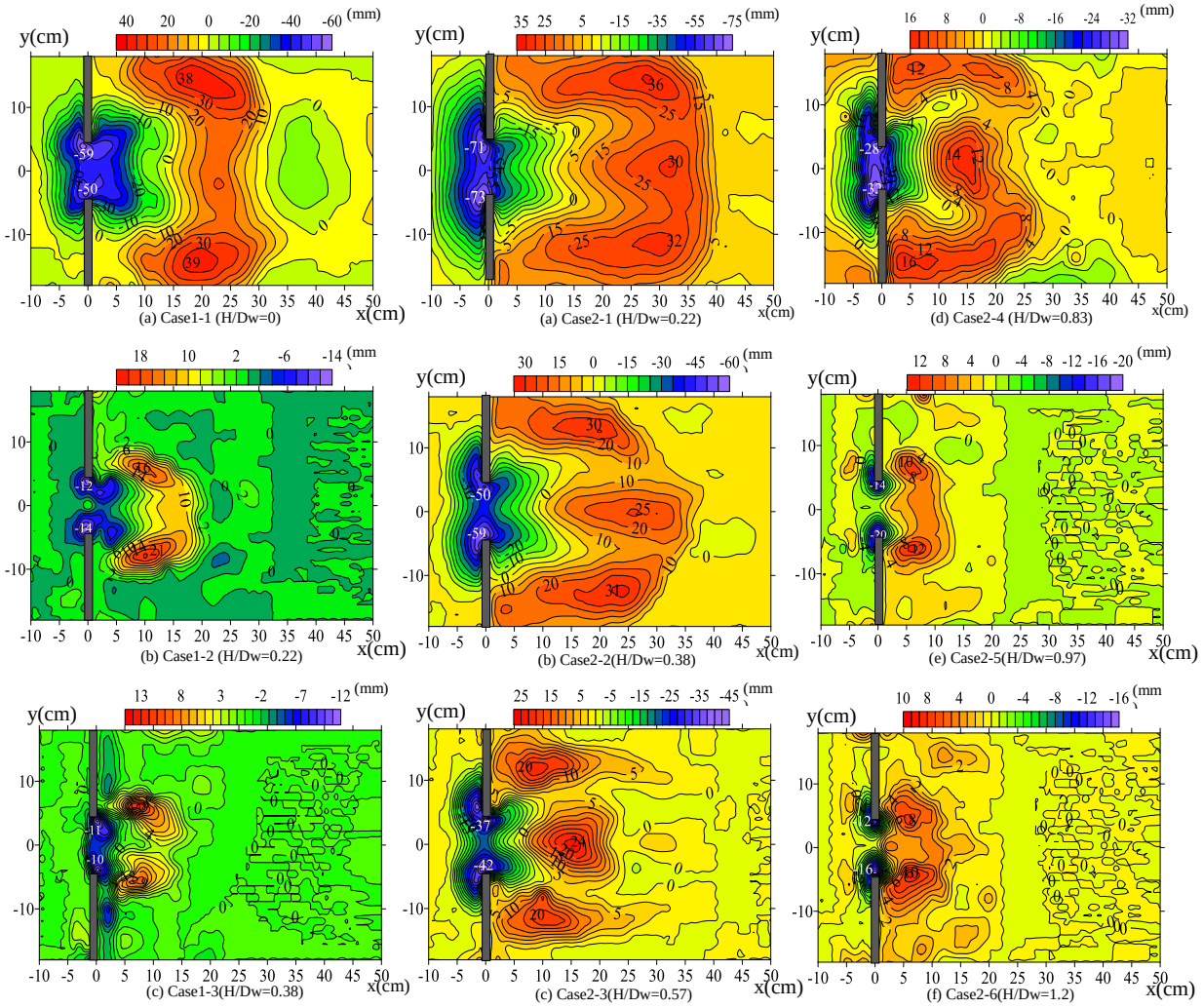

Figure 2. Bed deformation（ *U*=10cm/s）

Figure 3. Bed deformation（*U*=20cm/s）

side. It can be inferred that local scour becomes large in the areas where the downward flow due to the horseshoe-shaped vortices at the end to the weir meets the bed surface.

At the cross-sectional average flow velocity of 20 cm/s, conspicuous sandbars emerge in the mid-channel zone and near the right and left banks. The sandbars near the right and left banks are larger than the mid-channel sandbar, and their deposition patterns are similar within the relative overflow depth range from 0.22 to 0.83. At the relative overflow depths of 1.0 and 1.2, significant development of the mid-channel sandbar does not occur as in Case 1-2 and Case 1-3, because weir height is low and the main flow velocity near in the weir opening zone is low.

Figure 4 shows changes in maximum scour depth and maximum sediment thickness corresponding to different relative overflow depths. As shown, in a static equilibrium bed environment, the maximum scour depth and the maximum sediment thickness decrease exponentially as relative overflow depth increases. This suggests that as relative overflow depth increases, the rate and velocity of flow passing through the weir opening decrease relatively so that the velocity of flow approaching the weir decreases and horseshoe-shaped vortices at the end of the weir become weaker.

Figure 5 shows the longitudinal bed profile of the mid-channel zone at the cross-sectional average flow velocity of 20 cm/s. Figure 6 shows the transverse scour profile of the channel upstream of the weir. Figure 7 shows the transverse profile at the location where the maximum sediment thickness occurred in the region downstream of the weir.

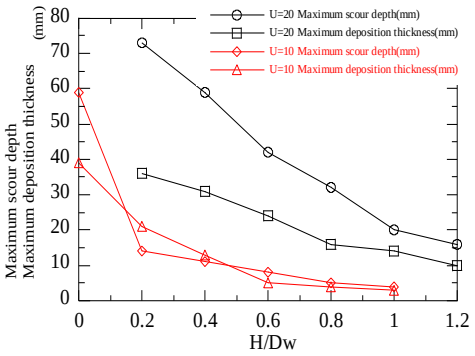

Figure 4. Maximum scour depth, Deposit Thickness and relative overflow depth

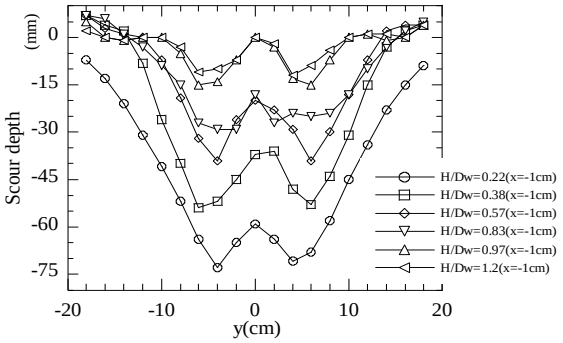

Figure 6. Scour profile upstream of overflow weir

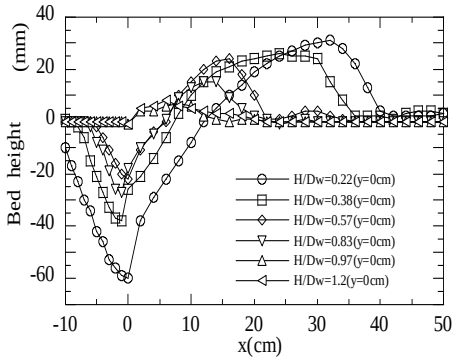

Figure 5. Longitudinal bed profile

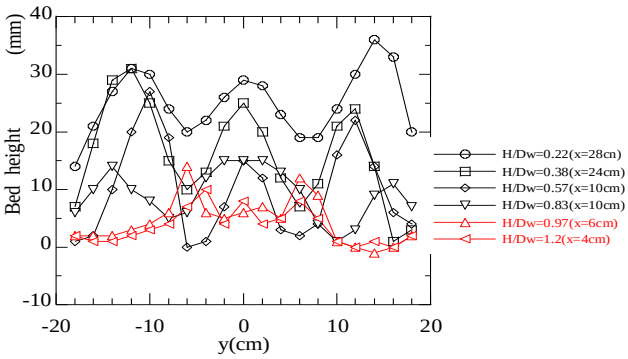

Figure 7. Cross-sectional bed profile

The mid-channel longitudinal profile of the bed is such that the scour slope angle upstream of the weir is 30° at a relative overflow depth of 0.2, 27° at 0.4 and 22° at 0.6, and the scour slope angle downstream of the weir is 21° at a relative overflow depth of 0.2, 21° at 0.4 and 18° at 0.6. These indicate that the scour slope angle decreases as the relative overflow depth increases and that the scour slope angle upstream of the weir is steeper than that the angle downstream of the weir and is close to the angle of repose (30°) in the case where the water is disturbed. The sediment deposition profile is such that the upstream slope is less steep than the downstream slope, and the downstream slope does not change significantly within the relative overflow depth range of 0.22 to 0.83 and remains around 22°.

The scour profile immediately upstream of the weir invariably shows a similar (W-shaped) pattern. Scour depth is maximized at the end of the weir (y = ±5 cm). The surface profile shows a rise at the center of the opening (y = 0 cm), and the scouring tendency becomes weaker as the relative overflow depth increases.

The transverse profile at the location where the maximum sediment thickness occurred in the region immediately downstream of the weir is as follows. Within the relative overflow depth range of 0.22 to 0.83, peaks can be seen at three locations: y = 0 cm and y = ±12 cm. It can also be seen that a valley-like area exists at y = ±6 cm. Within the relative overflow depth range of 0.97 to 1.2, there is a peak around y = ±6 cm, and there is a valley at y = 0 cm.

It can be inferred from the bed profile that strong horseshoe-shaped vortices occurred in front of the weir and downward flow occurred at the end of the weir opening, and, as a result, scour depth was maximized. It is thought likely that within the relative overflow depth range of 0.22 to 0.83, the horseshoe-shaped vortices occurring at the weir opening interfere with one another, and upward flow occur in the mid-channel zone where a peak is formed on the downstream side of the opening.

3.2. Local Flow on the Downstream Side of the Weir Opening

Figures 8 and 9 show the water surface and main flow velocity contours in Case 2-4. The water surface elevation is measured from the reference surface defined at the center of the channel at a point 3 m upstream from the weir and is shown in millimeters as a deviation from the reference surface. The contour diagram for main flow velocity also shows a streamline with a solid line. The water surface rises at the upstream face of the weir because of the backwater effect

and becomes relatively low at the downstream face of the weir. As shown, the water surface is locally high near the weir opening and shows large values in the regions immediately upstream of the weir at y = ±5 cm.

As shown, on the upstream side of the weir, high flow velocity zone where surface flow velocity Us is higher than 20 cm/s occurs at y = ±12 cm, and it gradually becomes narrower in the flow direction until its width decreases to y = ±5 cm at x = 40 cm. In the regions near both banks in the section downstream of the weir, low flow velocity zones become wider in the flow direction.

It can be seen that the streamlines of the surface flow also converge toward the center of the channel. The reason why the contour pattern is noticeably deformed in the mid-channel zone (x = 0 to 25 cm) is that the water surface changed considerably to the extent of showing a wavy pattern.

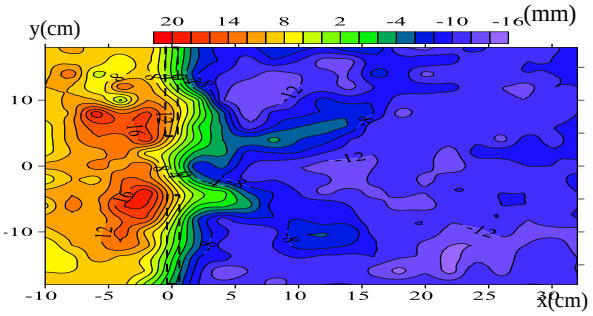

Figure 8. Water surface profile

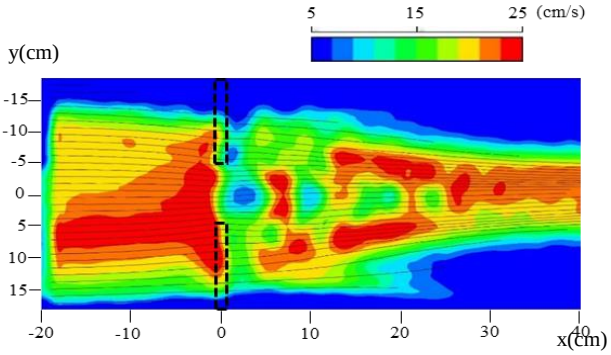

Figure 9. Free-surface velocity Us and stream line

Figures 10 to 12 show the plan view profiles of the main flow velocity (U) and the transverse (V) and vertical (W) components of secondary flow measured at 2 cm and 3.5 cm below the water surface. The crest of the weir is 2.5 cm below the water surface level.

The main flow velocity U tends to show large values in the sections upstream and downstream of the weir opening (y = −5 cm to +5 cm). The main flow velocity at 2 cm below the water surface, which is the region above the weir crest, is as follows. Except in the region upstream of the weir, the high flow velocity zone in the section upstream of the weir, where the cross-sectional average flow velocity is higher than 21.5 cm/s and U is higher than 22 cm/s, gradually becomes narrower in the flow direction. In the section downstream of the weir, the high flow velocity zone shows a pattern similar to the pattern of the surface flow and tends to gradually become narrower in the flow direction. It can also be seen that the flow velocity in the sections upstream and downstream of the weir is relatively high because of the influence of the overflow. The low flow velocity zones near the right and left banks downstream of the weir tend to gradually become wider.

The main flow velocity at 3.5 cm below the water surface, which is a region below the weir crest, is as follows. In the section upstream of the weir, the high flow velocity zone, where U is higher than 22 cm/s, sharply becomes narrower and accelerates toward the weir opening. In the section downstream of the weir, it sharply becomes wider and decelerates. The low flow velocity zones near the right and left banks tend to sharply become narrower.

It can also be seen that low flow velocity zones emerge over the sandbars formed along the right and left banks downstream of the weir. The region over the mid-channel sandbar, which is located directly downstream of the opening, shows a tendency to decrease in the section corresponding to x = 10 to 30 cm.

The transverse component V and vertical component W of the secondary flow show similar tendencies although there are certain differences between 2 cm and 3.5 cm below the water surface. In the section upstream of the weir, the transverse component V of the secondary flow is a flow that tends to converge while advancing toward the weir opening and shows a maximum value at y = ±5 cm immediately upstream of the weir. In the section downstream of the weir, the transverse component shows a maximum value at 5 cm immediately downstream of the weir. As shown, in the section downstream of the weir, there is convergent flow moving toward the weir opening. In the regions over the sandbars downstream of the weir, there is divergent flow of the transverse component V of the secondary flow in

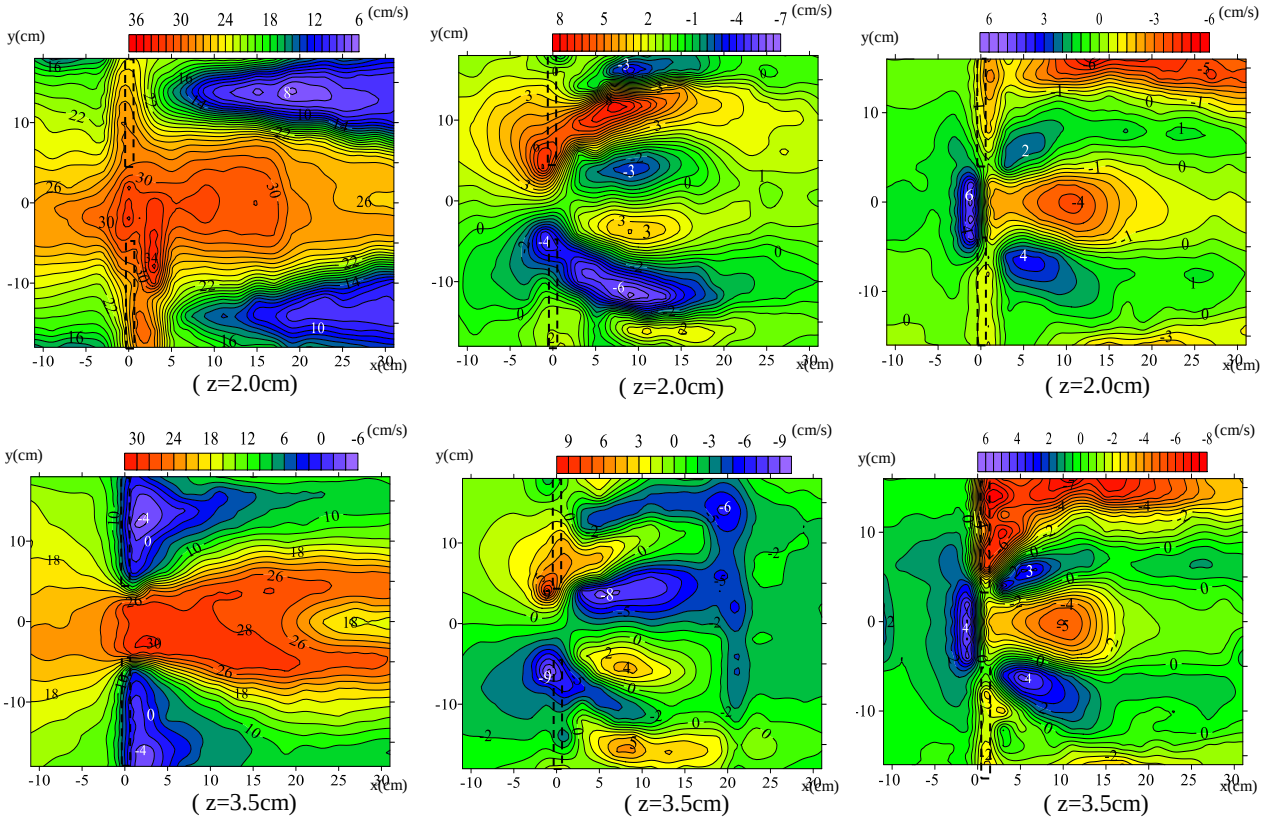

Figure 10. Plan view profiles of main flow velocity (U)

Figure 11. Plan view profiles of transverse velocity (V)

Figure 12. Plan view profiles of vertical velocity (W)

the peak regions. In the valley regions between the sandbars, there is divergent flow. In the section downstream of the weir, the location of the vertical component W of the secondary flow is strongly related to the sandbar locations, and W tends to show upward flow in the regions over the sandbars and convergent downward flow in the regions between the sandbars.

Figures 13 and 14 show vertical contours of the vertical component W of the secondary flow and the main flow velocity U at x = 10 cm, x = 20 cm, and x = 30 cm in the section downstream of the weir, respectively.

The vertical component W of the secondary flow shows a spatial distribution with a very high degree of regularity. As shown, upward flow occurs at around y = 0 cm (mid-channel zone) and y = ±15 cm, and downward flow occurs in the sections of y = −10 cm to −5 cm and y = 3 cm to 8 cm, which correspond to the valleys between the sandbars. As shown, the horseshoe-shaped vortex oriented transversely along the weir gradually changes its orientation into a longitudinal vortex oriented in the flow direction as it flows downstream through the weir opening, and longitudinal vortices rotating in the opposite direction are formed around the central vortex. From the sizes of the upward and downward currents, it can be inferred that the intensity of those vortices is maximized at x = 10 cm and becomes somewhat weaker as the water flows downstream.

The diagram showing the contours of the main flow velocity U also shows secondary flow cells, identified by referring to Figures 11 to 13, with a broken line. The main flow velocity U is relatively high and uniform in spatial distribution in the weir opening zone (y = −5 cm to +5 cm), and the maximum flow velocity tends to decrease slightly in the flow direction. At x = 20 cm and x = 30 cm, the main flow velocity contours show an upwardly convex shape near the bottom and a downwardly convex at around y = ±5 cm. This is thought to be because of the upward flow in the mid-channel zone and the downward flow at around y = ±15 cm.

The main flow velocity of weir crest overflow in the sections y = −18 cm to −5 cm and y = +5 cm to +18 cm is

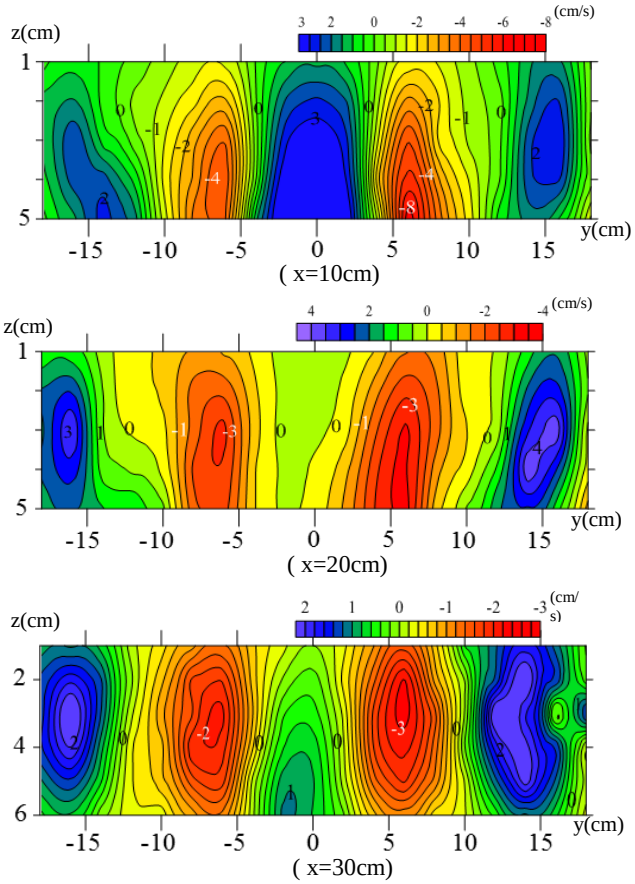

Figure 13. Cross-sectional profiles of vertical velocity (W)

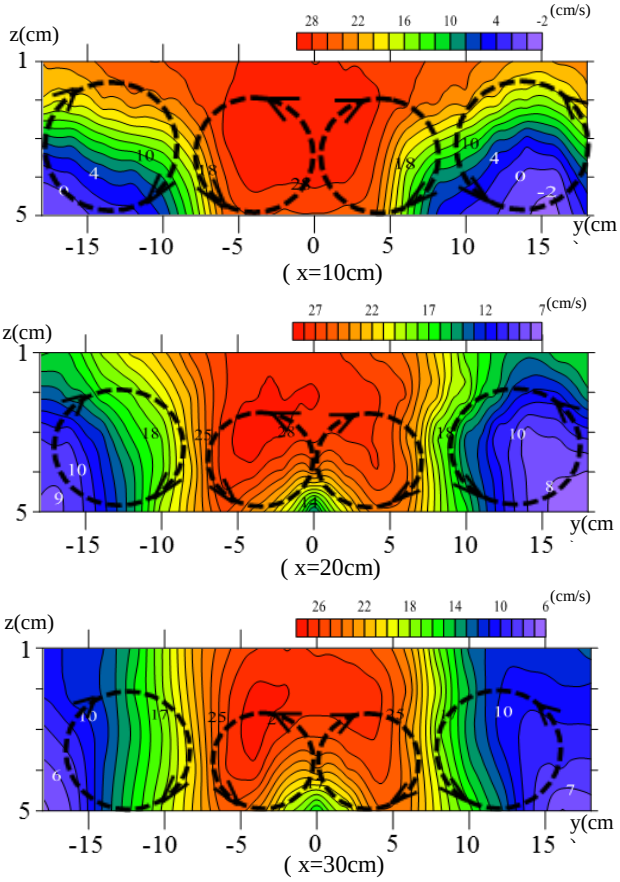

Figure 14. Cross-sectional profiles of main flow velocity (U)

relatively low. At x = 10 cm, vertical spatial changes in main flow velocity are large under the influence of the weir, and strong shear layers are formed. As the water flow downstream, vertical changes become smaller, and velocity changes in the transverse direction become increasingly conspicuous. In the sections y = −18 cm to −13 cm and y = 13 cm to 18 cm, flow velocity in the near-surface zone tends to decrease as the water flows downstream. This indicates that low-velocity fluid masses near the bottom were moved up toward the water surface zone by the strong upward currents along the right and left banks. At around y = ±10 cm, a deceleration tendency is shown in the near-surface zone and a slight acceleration tendency can be seen in the near-bottom zone. It is to be noted that at x = 30 cm, flow velocity tends to be higher in the near-bottom zone than in the near-surface zone, though only slightly. This, too, can be explained by the momentum transport by the secondary flow induced by spiral flow.

4. Conclusion

Focusing on a static equilibrium river bed environment, this study looked at the effect of a weir with an opening on the river bed processes downstream and the three-dimensionality of flow over sandbars formed in the section downstream of the weir. Main findings of this study are as follows:

1) Scouring of a weir with an opening occurs mostly around the opening and the two-dimensional spread and depth of scour become smaller as the relative overflow depth increases.

2) In a static equilibrium river bed environment, the maximum scour depth and the maximum sediment thickness decrease exponentially as the relative overflow depth increases.

3) The cross-sectional profile of scour in the section immediately upstream of the weir invariably shows a similar W-shaped pattern. Scour depth is maximized at the end of the weir, and the bed profile show a rise in the mid-channel zone. The scouring tendency becomes weaker as the relative overflow depth increases.

4) The location of the maximum sediment thickness in the transverse direction in the section downstream of the weir is as follows. Within the relative overflow depth range of 0.22 to 0.83, a peak occurs at three locations, namely, y = 0 cm and y = ±12 cm, and a valley occurs at around y = ±6 cm.

5) On the upstream side of the weir, strong downward flow occurs near the weir opening. In the section upstream of the weir, under the strong locational influence of sandbars, upward flow was observed in the regions over the sandbars, and convergent upward flow was observed in the valleys between the sandbars.

6) The horseshoe-shaped vortex oriented transversely along the weir gradually changed its orientation into a longitudinal vortex oriented in the flow direction as it flowed downstream through the weir opening, and longitudinal vortices rotating in the opposite direction were formed around the central vortex.

5. Acknowledgements

The authors would like to address their sincere thanks to the Arase dam removal technical research committee and Kumamoto prefectural government for providing valuable data.

6. References

M.W., Doyle, E.H.Stanley, Orr, C.H., Selle, A.R., Sethi, S.A. and Harbor, J.M. (2005). "Stream ecosystem response to smalldam removal: lessons from the Heartland," *Geomorphology*, 71, pp. 227-244.

Amy E. East (2015). "Large–scale dam removal on the Elwha River," Washington, USA: River channel and floodplain geomorphic change, *Geomorphology*, 228, pp. 765-786.

W. L. Graf, Editor (2002). Dam Removal Research - Status and Prospects-, THE H. JOHN HEINZ III CENTER FOR SCIENCE, ECONOMICS AND THE ENVIRONMENT

T. Ishigaki and Y. Baba (1999). "Flow Structure and Local Scour around a Plate with Footing," *Journal of applied mechanics*, JSCE, Vol. 2 (1999) P 657-664 (in Japanese)

K. M.Kibler, D. D. Tullos, and G. M. Kondolf (2011). "Learning from dam removal monitoring: challenges to selecting experimental design and establishing significance of outcomes," *River Research and Applications*, Vol.27, pp.967-975.

Bruce W. Melville (1997). "Pier and Abutment Scour. Integrated Approach," *J. Hydraulic Engineering*, ASCE, Vol.123, No.2, pp.125-136.

Guan, D., Melville, B., and Friedrich, H. (2013). "Flow Patterns and Turbulence Structures in a Scour Hole Downstream of a Submerged Weir," *J. Hydraulic Engineering*, Vol.140, No.1, pp.68-76.

T. Ohmoto and R. Hirakawa (1999). "Three-dimensional Structures in an Open Channel Flow with a Series of Submerged Groynes," *Journal of applied mechanics*, JSCE, Vol. 2, P 665-672 (in Japanese).

Pagliara et al. (2016). "Scour due to rock sills in straight and curved horizontal channels," Journal of Hydro-environment research, 10, 12-20.

Rosgen, D. (2001). "The Cross-Vane, W-Weir and J-Hook Vane Structures...Their Description, Design and Application for Stream Stabilization and River Restoration," PROCEEDINGS of Wetlands Engineering & River Restoration Edited by Donald F. Hays, pp. 1-22, doi: 10.1061/40581(2001)72.

H. Sumida, Y. Muto, T. Tamura (2015). "Channel to Development on Upstream due to Change of Partially Removed Weir," *Journal of Japan Society of Civil Engineers*, JSCE, Ser. B1 (Hydraulic Engineering) Vol. 71, No. 4 p. I_925-I_930 (in Japanese)

Task Committee for the Arase Dam Removal in Enterprise Bureau of Kumamoto Prefectural Government (2017). <http://www. Arase damtekkyo.hinokuni-net.jp/02_page/05_kyougikaitou/>, (in Japanese)

Zhang H., Muto, Y., Nakagawa, H and Nakanishi, S. (1999). "Weir removal and its influence on hydro-morphological features of upstream channel," *Journal of applied mechanics*, JSCE, Vol.15, No2, pp.591-599.